ROMANIAN ACADEMY
"ILIE MURGULESCU" Institute of Physical Chemistry
BUCHAREST

PhD thesis

SUPRAMOLECULAR SYSTEMS INVESTIGATED BY DUAL PARAMAGNETIC AND FLUORESCENT MOLECULAR PROBES

Scientific coordinator,
Dr. Elena Gabriela Ioniță

PhD student,
Mocanu Sorin

2019

Table of contents

Key words: Electron paramagnetic resonance spectroscopy (EPR), Fluorescence spectroscopy, molecular probes, Cyclodextrins, Pluronic

INTRODUCTION

The thesis is structured in two chapters. The **first chapter** provides a general overview in the field of supramolecular chemistry, with a special focus on host-guest systems. The fundamentals and recent advances in the fields of electronic paramagnetic resonance (EPR) and fluorescence spectroscopy are presented as well. The EPR and fluorescence parameters reported in literature and their application to the characterization of host-guest inclusion complexes are discussed. In addition, the studies reported in literature on dual fluorescent and paramagnetic probes are reviewed.

Chapter two presents the original contribution that refers to the synthesis of two new series of dual molecular probes, and their utility in characterizing supramolecular systems such as host-guest systems. We also analyse the behaviour of these dual probes upon diffusion in polymeric gels, and their use in highlighting the chemical processes occurring in hybrid materials represented by hybrid polymeric gels that encapsulate gold nanoparticles.

The first series of dual molecular probes have in their structure the pyrene fluorescent moiety and TEMPO paramagnetic moiety linked by oligo-ethylene glycol chains.

The second series of compounds with fluorescent and paramagnetic properties have as structural units the dansyl and TEMPO moieties linked by alkyl chains.

The properties of these dual molecular probes were compared with those of the corresponding mono-molecular fluorescent derivatives. Another study refers to the properties of a series of bis-dansyl derivatives obtained as secondary products, and to their interaction with cyclodextrins.

The data reported in this thesis are included in three published articles, a manuscript sent for evaluation, and a manuscript in preparation.

The last chapter summarizes the conclusions and perspectives for further research in this field.

CHAPTER II
ORIGINAL RESULTS

The main objective of this thesis was to investigate supramolecular systems of varying degrees of complexity, in which cyclodextrins are constitutive elements, by using dual, paramagnetic and fluorescent, molecular probes.

The studies were oriented towards the synthesis of two series of dual molecular probes in which the paramagnetic moiety is connected to the fluorescent moiety by a linear, flexible chain. We focused on the analysis of how the spectral parameters of the two moieties, paramagnetic and fluorescent, mutually influence each other, as a function of the characteristics of the flexible linker.

In the case of the first series of dual molecular probes, the paramagnetic TEMPO moiety is connected to the fluorescent pyrene moiety *via* oligo-ethylene glycol chains.

In the case of the second series, the paramagnetic TEMPO moiety is connected to the fluorescent dansyl moiety by alkyl chains. In addition to these dual probes, we also obtained mono- and bis-dansyl fluorescent derivatives.

The newly-synthesised compounds were purified using thin layer chromatography (TLC), and characterized using gas chromatography, IR spectroscopy, NMR spectroscopy (in the case of the diamagnetic probes), EPR and fluorescence spectroscopies.

The interaction of the probes with cyclodextrins in solution was evidenced by changes in the EPR and fluorescence spectral parameters. The host-guest interaction with cyclodextrins was also shown to occur in hydrogels that contain cyclodextrins in their covalent network. In the case of dual probes bearing oligo-ethylene glycol chains as linkers, EPR and fluorescence parameters were analysed in order to evidence the micelle-to-gel phase transition occurring in systems that contain Pluronic F127, in the presence or in the absence of cyclodextrins.

An interesting chapter refers to the analysis of the processes that occur in hydrogels upon the formation of metallic gold nanoparticles by reduction of a gold salt in hydrogel. Nanoparticle formation is accompanied, in a first step, by the decrease of the EPR signal and increase of the fluorescence emission, followed in time by the partial recovery of the EPR signal.

II.1. Dual molecular probes in which the TEMPO paramagnetic moiety and pyrene fluorescent moiety are linked by oligo-ethylene glycol chains

In order to investigate in detail the correlation between the spectral parameters of dual molecular probes and the structural characteristics of the flexible linker, we selected a series of oligo-ethylene glycols to connect pyrene, as fluorescent moiety, with TEMPO, as paramagnetic moiety.

The choice of pyrene as fluorophore was based on the existence of an impressive number of studies in which pyrene and its derivatives are used as fluorescent probes to investigate processes involving molecular assembly [1-4]. It is well known that the fluorescence spectrum of pyrene is characterised by a vibrational structure sensitive to local changes in polarity and dynamics. The experimental parameter used to characterise the system is the ratio between the intensities of bands I and III in the pyrene spectrum [1-6].

It is possible for the fluorescence spectrum of pyrene derivatives to lack the characteristic vibrational structure. A number of studies report the synthesis of such derivatives that bear alkyl chains attached to the pyrene moiety. Pyrene derivatives, including pyrene attached to polyethylene glycols, were further attached to macromolecules in order to study the properties of the latter [1, 7-9]. There is however no report on a series of derivatives in which the pyrene fluorophore is attached to oligo-ethylene glycol chains. One study reported a compound in which a tetraethylene glycol chain is attached to pyrene [1].

Compounds bearing two paramagnetic TEMPO moieties attached to oligo-ethylene glycol chains were reported in the literature [10], the experimental data indicating a non-linear dependence of the EPR lines attributed to the exchange interactions on the length of the oligo-ethylene glycol chain. These observations prompted us to perform the synthesis of novel dual molecular probes with TEMPO and pyrene moieties connected by oligo-ethylene glycol chains.

II.1.1. Synthesis and characterisation of $Py(EG)_nT$ dual molecular probes

Dual molecular probes in which the TEMPO paramagnetic and pyrene fluorescent moieties are connected by oligo-ethylene glycol chains were synthesised by a two-step procedure, as shown in figure 1.

In the first step, oligo-ethylene glycol was reacted with 1-pyrenecarboxylic acid in the presence of DCC and DMAP with the formation of the fluorescent derivative, noted as $Py(EG)_n$.

In the second step of the synthesis, $Py(EG)_n$ was reacted with 4-carboxy-TEMPO in dichloromethane in the presence of the same coupling agent (DCC) and the DAMP base.

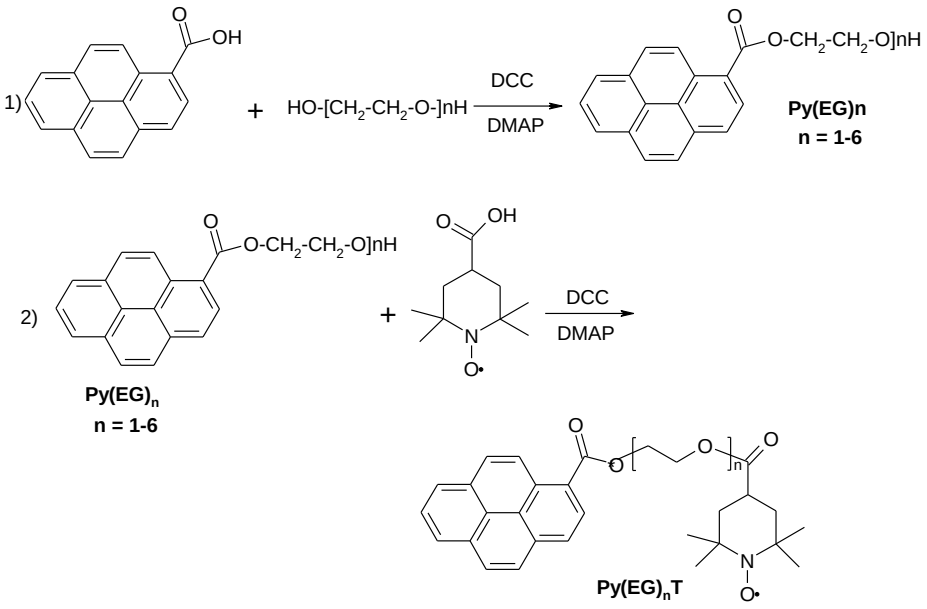

Fig. 1. Reaction of 1-pyrenecarboxylic acid with oligo-ethylene glycol to obtain the fluorescence compounds $Py(EG)_n$, followed by their reaction with 4-carboxy-TEMPO to obtain the dual molecular probes $Py(EG)_nT$

The molecular probes were characterised by TLC, mass spectrometry, EPR, fluorescence, IR spectroscopies and, in the case of the $Py(EG)_n$ probes, by NMR spectroscopy as well.

EPR and fluorescence properties of the dual molecular probes Py(EG)$_n$T

The EPR parameters of the Py(EG)$_n$T probes were determined directly from the experimental spectra, since the latter indicate a fast dynamic with a quasi-isotropic motion (the three lines are narrow, with the third line wider and having a smaller intensity than the other two lines, figure 2). The smaller intensity of the third line is due to the fact that the paramagnetic fragment is attached to a much larger structure, the oligo-ethylene glycol chain.

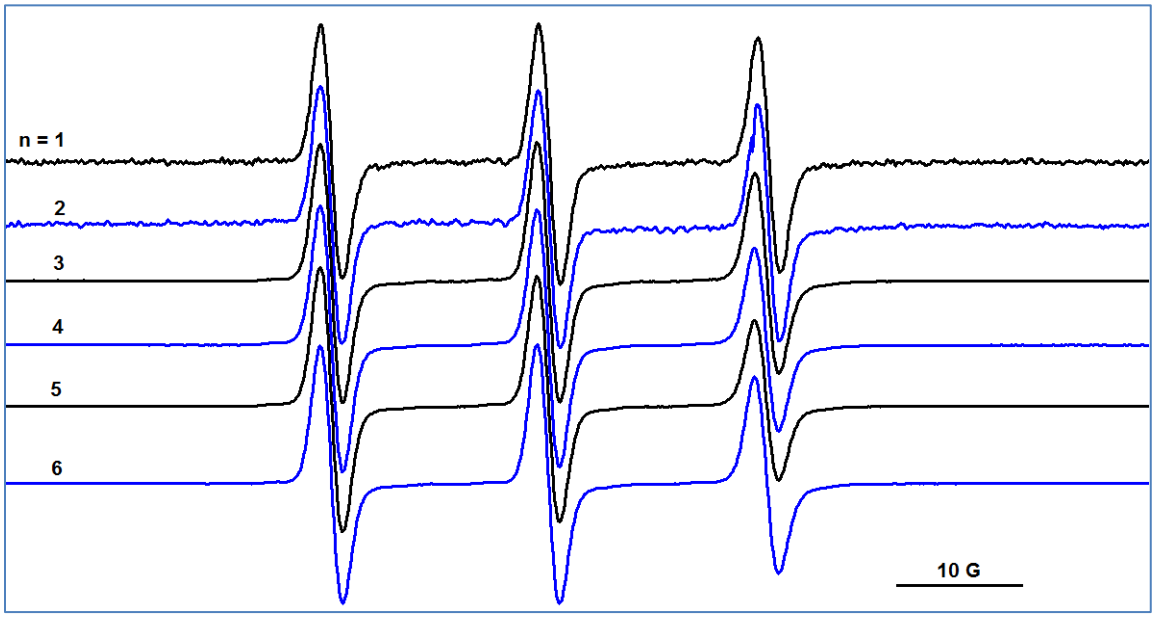

Fig. 2. EPR spectra of Py(EG)$_n$T probes in aqueous solution, at pH 7.4

From figure 3 it can be observed that the rotational correlation time, τ_c varies non-linearly with the length of the oligo-ethylene glycol chain in the interval $(0.3–1.5)\times10^{-10}$ s. Normally, we expect a linear increase of the rotational correlation time with the molecular weight of the paramagnetic species in a series. The deviation from this behaviour in the case of Py(EG)$_n$T probes can be explained by the flexibility of the oligo-ethylene glycol chain.

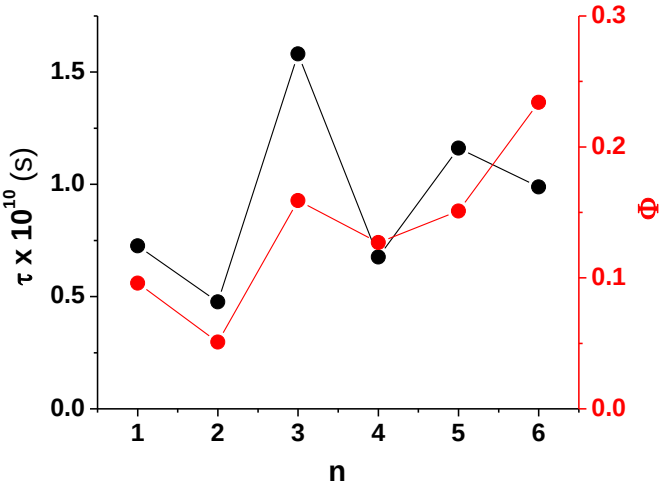

Fig. 3. The variation of the rotational correlation time (τ_c) and fluorescence quantum yield (Φ) of Py(EG)$_n$T dual probes with the length of the oligo-ethylene glycol chain (n).

From the analysis of the EPR data, it was observed that the nitroxide group in the probes bearing an even number of ethylene oxide groups is characterised by a faster rotation motion. Regarding the emission properties of the probes, a lower fluorescence emission was recorded for the Py(EG)$_n$T derivatives as compared to the Py(EG)$_n$ parent compounds, due to the TEMPO moiety attached to the oligo-ethylene glycol chains acting as fluorescence quencher.

The fluorescence quantum yields of the Py(EG)$_n$ probes are ~0.56 irrespective of the length of the oligo-ethylene glycol chain. In contrast, the quantum yield values of the Py(EG)$_n$T dual probes vary significantly depending on the chain length (from 0.23 for n = 6 to 0.05 for n = 2) due to the different proximity of the fluorophore with the nitroxide quencher, which is determined by the conformation and length of the oligo-ethylene glycol chain. As can be observed from figure 3, Py(EG)$_2$T has the lowest fluorescence quantum yield, indicating that the most stable chain conformation brings the two end groups closer to each other. The ratio between the fluorescence band area of each sample and the fluorescence band area of 1-pyrenecarboxylic acid represents a measure of the magnitude of intermolecular quenching due to the paramagnetic moiety.

The non-linear behaviour of EPR and fluorescence parameters can provide distinct information in complex systems in which host-guest interactions occur, or in block copolymer micelles where the hydrophilic/hydrophobic properties are non-uniform.

II.1.2. Non-covalent interactions of $Py(EG)_{nT}$ dual molecular probes

II.1.2.1. Interaction with β-cyclodextrin in solution

In order to evidence the formation of host-guest complexes between $Py(EG)_nT$ dual probes and β-CD, we recorded the EPR and fluorescence spectra of the probes in a series of solutions containing β-CD in the concentration range 10^{-5}–10^{-2} M. The spectral (EPR and fluorescence) parameters were then used to obtain thermodynamic data (association constants, stoichiometry of the complexes), as well as information on the geometry of the host-guest complexes formed.

The hyperfine splitting constant (a_N) is the EPR parameter employed to evidence local polarity changes in the vicinity of the paramagnetic group. For the $Py(EG)_nT$ series of probes, this parameter varies non-uniformly. For dual probes bearing short oligo-ethylene glycol chains, namely $Py(EG)_1T$ and $Py(EG)_2T$, we observe a decrease in the a_N value that is proportional to the increase in the β-CD concentration. The maximum changes in $2a_N$, corresponding to a β-CD concentration of 10^{-2} M, were of 1.12 G and 0.67 G for $Py(EG)_1T$ and $Py(EG)_2T$, respectively (figure 4).

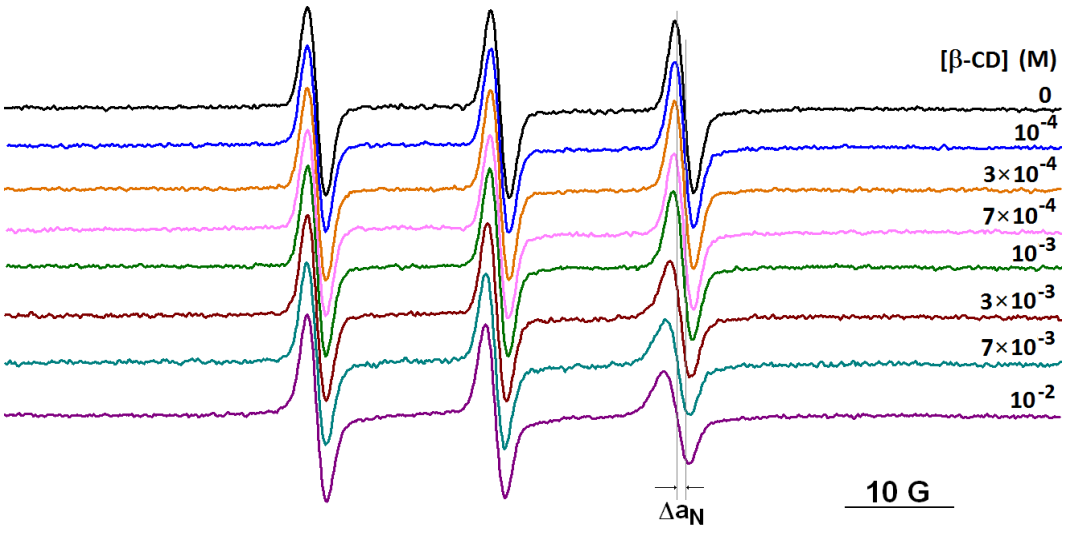

Fig. 4. The EPR spectrum of $Py(EG)_2T$ recorded at 20°C in the absence and in the presence of β-CD

Differently from the case of $Py(EG)_1T$ and $Py(EG)_2T$, the a_N value of the superior terms of the series of probes is less sensitive to the presence of β-CD. This different behaviour suggests different geometries of the host-guest complexes formed by the first two terms of the series as compared to the superior terms. In the case of $Py(EG)_1T$ and $Py(EG)_2T$, complexation most probably involves the inclusion of the nitroxide moiety in the β-CD hydrophobic cavity. This is supported by the significant decrease of the a_N value in the presence of β-CD, which is indicative of a less polar microenvironment sensed by TEMPO.

In order to enrich the information obtained by EPR spectroscopy, we recorded and analysed the fluorescence spectra of $Py(EG)_nT$ dual probes, as well as the spectra of $Py(EG)_n$ fluorescent probes, in β-CD solutions in the concentration range 10^{-5}–10^{-2} M. It was observed that the fluorescence spectra of these probes are sensitive to the presence of cyclodextrin, the general trends being similar for all probes to the one depicted in figure 5 for $Py(EG)_4T$. For β-CD concentrations up to 5×10^{-4} M, the fluorescence intensity decreases upon cyclodextrin addition. As the host concentration increases, two spectral features can be noted: 1) the appearance of the vibrational structure of the emission band, and 2) a hypsochromic shift of the emission band of ~20 nm at maximum β-CD concentration.

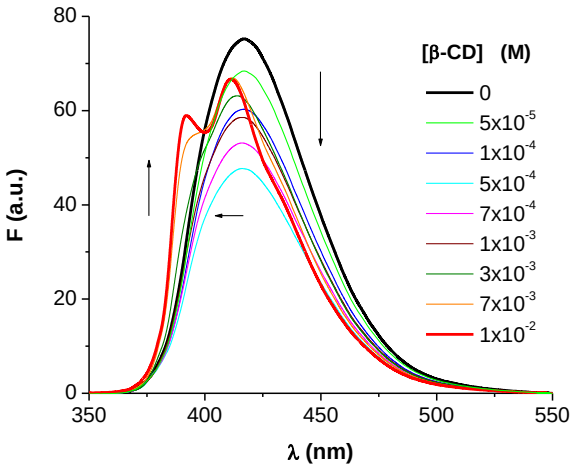

Fig. 5. Steady-state fluorescence spectra of $Py(EG)_4T$ in the absence and in the presence of increasing concentrations of β-CD

The changes observed in the fluorescence spectra of the probes are significantly different from those frequently reported in the literature [11]. Thus, we can assume a different interaction mechanism in our case. Host-guest complexes of cyclodextrins involve either inclusion of the guest in the β-CD cavity or encapsulation of the guest by host molecules. These two types of complexes are schematically represented in figure 6.

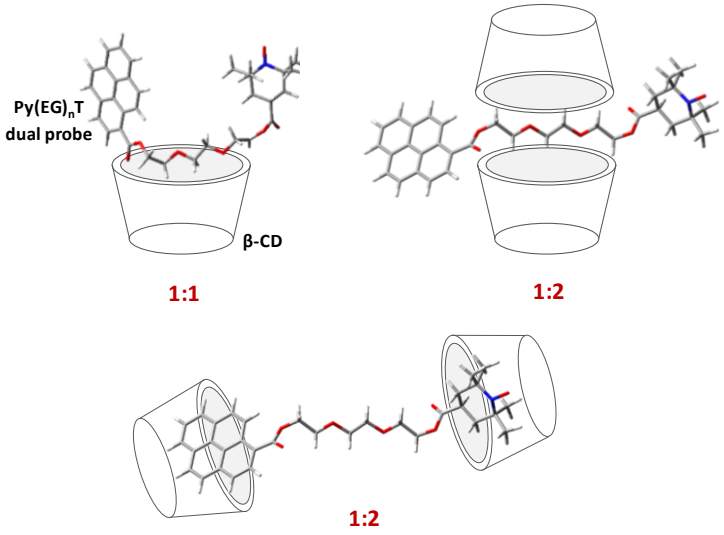

Fig. 6. Schematic representation of the geometries of inclusion and excapsulation complexes with 1:1 and 1:2 stoichiometries.

The association constants evaluated from the varation of spectral parameters with the β-CD concentration are of the order of magnitude 10^{-2} M for a 1:1 stoichiometry.

II.1.2.2. Diffusion of dual probes in polymeric gels containing β-cyclodextrin

Cyclodextrin molecules are characterised by an unrestricted motion in solution. However, there are systems that contain cyclodextrins fixed within a matrix. This is the case of covalent hydrogels formed by the reaction of isocyanate-functionalized polyethylene glycols with cyclodextrins [12-15]. The synthesis and structure of such a covalent gel network are depicted schematically in figure 7. The effects of the presence of cyclodextrin molecules in the nodes of the gel network have been investigated. For this purpose, cyclodextrin was replaced with polyalcohols (such as glycerol or pentaerythritol)

in the synthesis of hydrogels, in order to form covalent polymeric networks while simultaneously excluding the possibility of formation of host-guest complexes inside the gel [13].

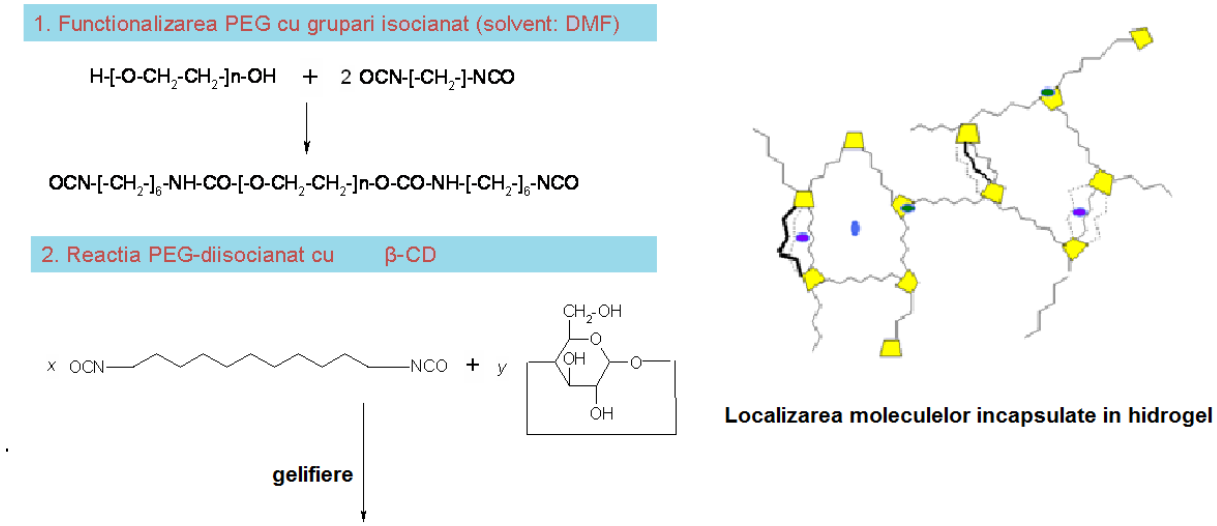

Fig. 7. Two-step preparation of polymeric hydrogels and schematic representation of their structure

Starting from the features of the Py(EG)$_n$T dual probes in interaction with β-CD, as described above, we recorded EPR and fluorescence spectra of Py(EG)$_1$T and Py(EG)$_6$T probes in two hydrogels. The first type of hydrogel was prepared by the reaction of PEG900 with β-CD, while the second type of hydrogen was obtained by the reaction of PEG900 with glycerol.

The diffusion of the Py(EG)$_n$T dual probes in these hydrogels ws evidenced in the EPR spectra by the presence of two component with different dynamic of the paramagnetic group. In the case of the PEG900/glycerol hydrogel, the EPR spectra of the dual probes show only one component, with a relatively fast motion [61]. Surprisingly, in the EPR spectrum of the dual probe Py(EG)$_6$T diffused into PEG900/glycerol hydrogel, one can observe the presence, in low proportion, of a second, immobilized component characterised by a strongly restricted motion (figure 8).

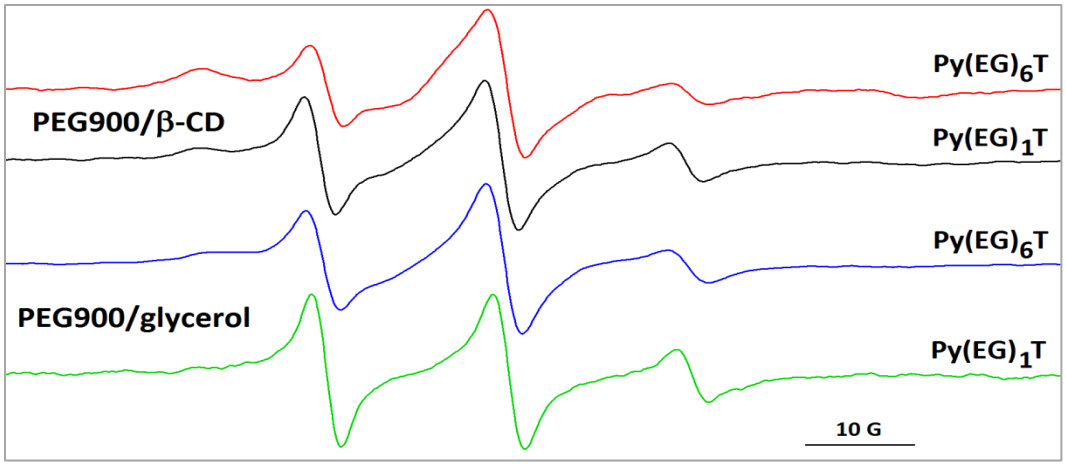

Fig. 8. The EPR spectra of Py(EG)$_1$T and Py(EG)$_6$T dual probes in PEG900/β-CD and PEG900/glycerol hydrogels.

These results point out to the fact that the dual molecular probes interact with gel fibres, most probably due to the similar structure of the linker with the polyethylene glycol chains of the hydrogel. In the case of the PEG900/β-CD hydrogel, the component with strongly restricted motion is in higher proportion, demonstrating the role played by β-CD in the complexation process. The component with faster dynamic can be ascribed to dual probes placed in the solvent pools occupying the pores of the hydrogel network.

The fluorescence spectra of Py(EG)$_n$T dual probes after diffusion in PEG900/β-CD and PEG900/glycerol hydrogels are characterised by the appearance of the vibrational structure. In the case of β-CD in solution, the appearance of the vibrational structure of pyrene was observed at concentrations above 3×10^{-3} M. The position of the emission band at higher wavelength (414 nm) is neither sensitive to the linker length nor to the hydrogel type. Differently, the emission band at lower wavelength is sensitive to the gel type. The most pronounced effect is observed for Py(EG)$_6$T and consists in a 3 nm hypsochromic shift. This is evidence of the interaction between the oligo-ethylene glycol linker and the polyethylene glycol chains in the gel fibres.

II.1.23. Redox processes in PEG/β-CD hydrogels containing gold nanoparticles

The PEG/β-CD polymeric hydrogels can encapsulate not only organic molecules like dual molecular probes [16] or spin probes [13], but also inorganic salts [17]. Previously, the storage capacity of PEG900/β-CD and PEG900/glycerol gels for $[AuCl_4]^-$ was analysed [17], as well as the partial reduction of Au^{3+} ions in gel and the formation of gold nanoparticles. In the case of the PEG900/β-CD gel, nanoparticles were formed in the absence of a reducing agent.

The $Py(EG)_nT$ dual probe was diffused in a PEG900/β-CD gel previously embedded with gold salt. Prior to the formation of gold nanoparticles, the medium is strongly acidic, which prompts the reduction of the nitroxide group. This is evidenced by the disappearance of the RES signal (figure 9, blue spectrum). The black spectrum in figure 9 is the signal of the dual probe diffused in a gel in which reduction did not occur. Following reduction of the nitroxide group, it would be expected for the fluorescence of the dual probe to increase. However, the Au^{3+} ions are known fluorescence quenchers, therefore the formation of gold nanoparticles only leads to a small increase in the fluorescence intensity of the dual probe. The EPR signal of the dual probe is partially restored in time, indicating the oxidation of hydroxylamine to nitroxide occurring at the surface of gold nanoparticles.

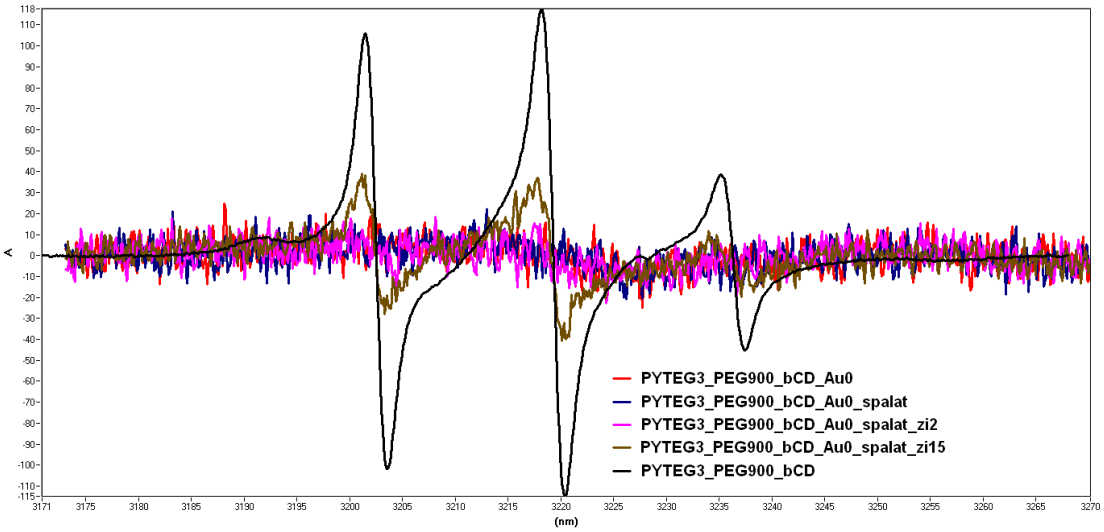

Fig. 9. The EPR spectrum of $Py(EG)_3T$ in PEG900/β-CD/Au^0 gel recorded at different time intervals

II.1.2.4. Behaviour of dual molecular probes in block-copolimer F127 systems

Block-copolymers of the type polyethylene oxide (PEO)-polypropylene oxide (PPO)-polyethylene oxide (PEO), also known as Pluronics or poloxamers, have the property to form micelles and gels within specific temperature and concentration intervals (figure 10) [18,19]. The micelle-to-gel phase transition appears as a result of the progressive dehydration of PEO chains. The hydrophilic/hydrophobic balance is different on going from the exterior towards the interior of micelles formed by Pluronics, and this property allows the controlled release of compounds encapsulated in micelles or in gel.

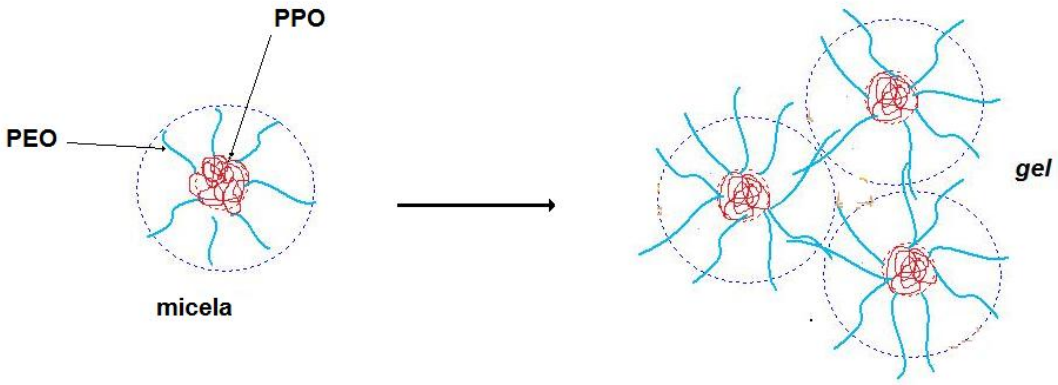

Fig. 10. Schematic representation of the structure of the Pluronic F127 micelle

Two series of monomolecular probes were used, paramagnetic ($(EG)_nT$, P3T2) or fluorescent ($Py(EG)_n$), as well as the dual molecular probes $Py(EG)_nT$ (figure 11), to evidence the changes occurring in systems containing Pluronic F127 at a concentration of 16,6%, in the absence and in the presence of increasing concentrations of 2-hydroxypropyl-β-cyclodextrin (HPB) [20].

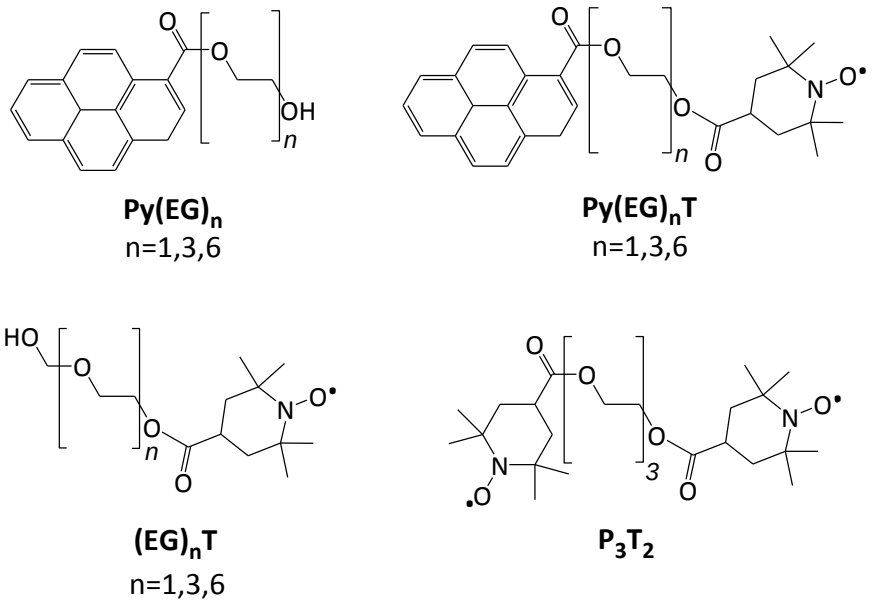

Fig. 11. Fluorescent probes, spin probes and dual molecular probes used in this study

Micelle-to-gel transition evidenced by fluorescence spectroscopy

The fluorescence spectra of the mono- and dual molecular probes $Py(EG)_n$ and $Py(EG)_nT$ were recorded in the temperature range 293-338 K with a step of 5 K, in two HPB solutions at different concentration and in three systems containing F127 and/or HPB (table 7).

Table 7. Sample composition, critical gelation point (cgt) and temperature interval of the gel domain (ΔT)

System	Composition	*cgt* (K)	ΔT (K)
F127-1	F127 16.6 wt. %	304.5	34
F127-2	F127 16.6 wt. % F127/HPB=1:0.6	305.3	33
F127-3	F127 16.6 wt. % F127/HPB=1:1.35	309.2	32
HPB-1	1.1% (7.5×10^{-3} M)	–	–
HPB-2	6.8% (4.6×10^{-2} M)	–	–

In HPB solutions, the fluorescence intensity of the probes decreases slightly, linearly with the temperature, as an effect of intermolecular collisions.

In the systems F127 1-3, the decrease in fluorescence intensity is significant in the temperature range analysed, as can be observed from figure 12.

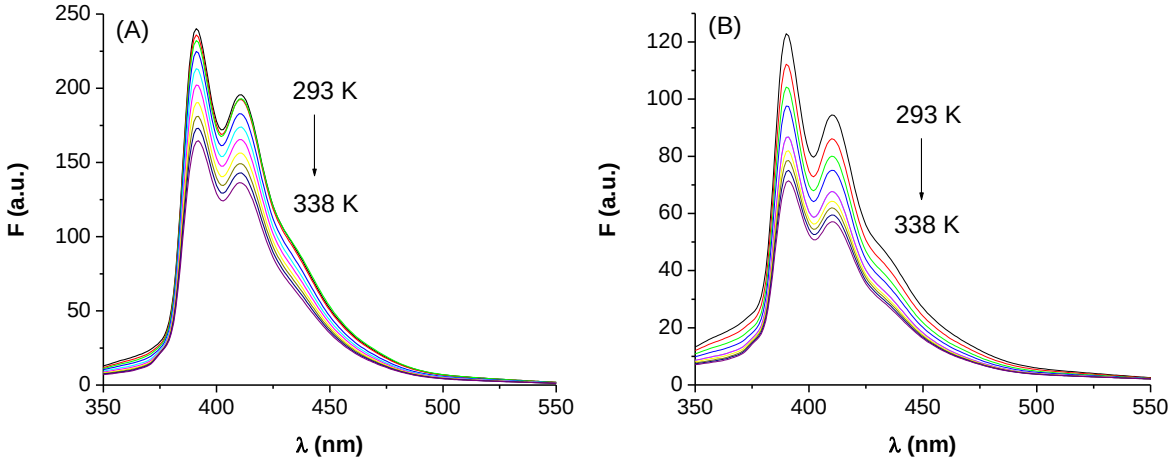

Fig. 12. Fluorescence spectra of (A) Py(EG)$_3$ and (B) Py(EG)$_3$T in F127-1 upon increasing temperature

The variation of the fluorescence intensity in the temperature range 293-338 K is non-linear. We noted a similar behaviour of probes Py(EG)$_n$ and Py(EG)$_n$T .

The phase transition temperatures were estimated from the curve indicating the variation of the ratio of fluorescence intensities at 390 and 410 nm with temperature, as the intersection of two imaginary lines connecting the points from temperatures corresponding to micellar phase and the points at higher temperatures. The results are given in table 8.

Table 8. Temperature of the micelle-to-gel transition (in K) reported by fluorescent probes in the systems F127 1-3

Probe	**Py(EG)$_1$**	**Py(EG)$_3$**	**Py(EG)$_6$**	**Py(EG)$_1$T**	**Py(EG)$_3$T**	**Py(EG)$_6$T**
F127-1	310	304	307	307	307	309
F127-2	312	307	304	307	310	308
F127-3	309	305	303	308	308	303

Micelle-to-gel transition evidenced by EPR spectroscopy

As opposed to the fluorescence data, the EPR spectral parameters of dual and paramagnetic probes $Py(EG)_nT$ and $(EG)_nT$ showed significant changes in Pluronic systems. This can be observed from analysing the hyperfine splitting constant values, which clearly indicate that the molecular probes can access different regions in the micellar systems F127 1-3. A longer ethylene oxide chain determines a more hydrophilic character of the probe, which is reflected in a_N value. Thus, for the F127-1 system, the a_N value of $Py(EG)_1T$ is 16.33 G while that of $Py(EG)_6T$ is 16.57 G (table 9).

Table 9. The a_N values (in G) of spin probes in F127 systems in micellar phase at 293 K and in HPB-1 and HPB-2 solutions

System	$Py(EG)_1T$	$Py(EG)_3T$	$Py(EG)_6T$	$(EG)_1T$	$(EG)_3T$	$(EG)_6T$
F127-1	16.33	16.68	16.57	15.84	16.38	16.69
F127-2	16.37	16.64	16.55	16.20	16.44	16.41
F127-3	16.35	16.54	16.54	16.47	16.55	16.43
HPB-1	16.89	16.96	16.93	16.95	17.04	16.98
HPB-2	16.68	16.85	16.88	16.97	16.76	16.76

The behaviour of $(EG)_nT$ spin probes is different from that of dual probes $Py(EG)_nT$. In micellar phase, a distribution of the spin probes between the different regions of the micelle can be observed. This is evidenced in the EPR spectrum by the presence of two components in the case of the systems containing F127 (figure 13).

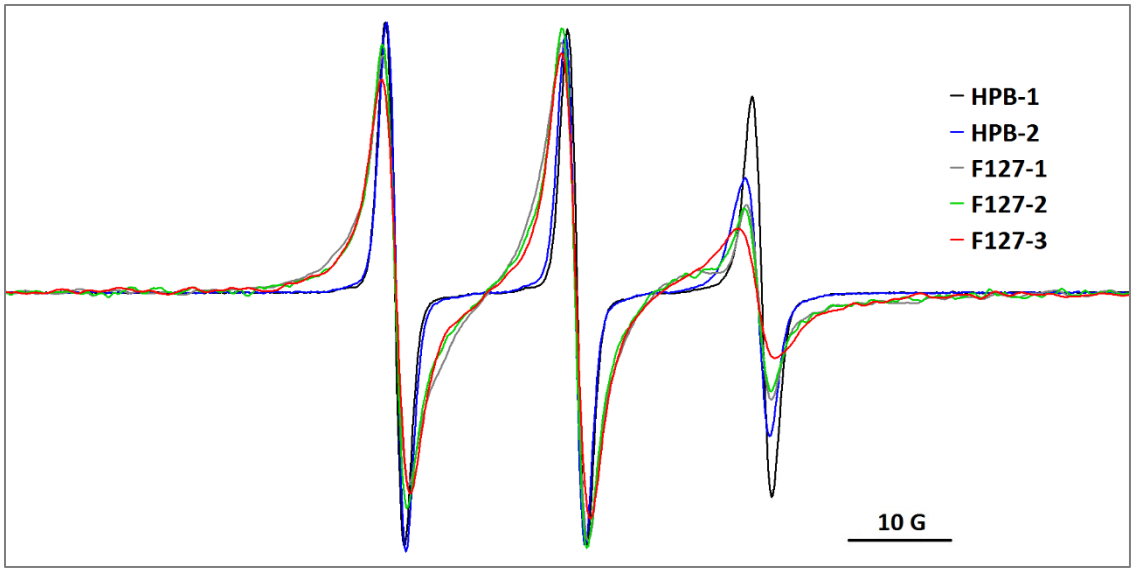

Fig. 13. The EPR spectra of $(EG)_3T$ in F127-1, F127-2, F127-3 and HPB-1, HPB-2 at 293 K

The P3T2 spin probe was selected to investigate F127 1-3 systems and HPB solutions in order to take advantage of the fact that the EPR lines ascribed to exchange interactions are influenced by probe complexation with cyclodextrin.

In conclusion, we can state that the structural particularities of the molecular probes greatly influence their response to the phase transition in Pluronic systems. The choice of investigation method is extremely important for such systems. Rheological methods yield macroscopic values of the critical gelation point and temperature interval of the gel, while spectral methods provide information at nanoscopic level. The fluorescence spectra of $Py(EG)_n$ şi $Py(EG)_nT$ are not sensitive to polarity changes. Differently, EPR spectra of all paramagnetic probes used in this study have shown changes of the hyperfine splitting constant, a_N, a parameter that is correlated to the local polarity. Therefore, EPR spectroscopy has allowed us to demonstrate that the gel formation process involves a continuous reorganisation in the temperature interval of the gel phase.

II.2. Dual molecular probes bearing the dansyl fluorescent moiety and TEMPO paramagnetic moiety linked by alkyl-diamine chains

II.2.1. Synthesis and characterization of $DA_{1.n}T$ dual molecular probes

The second series of dual molecular probes was synthesised in two steps by labelling linear 1,2-diamino alkanes with the dansyl fluorescent moiety and TEMPO paramagnetic moiety. The dual molecular probes have been noted as $DA_{1.n}T$.

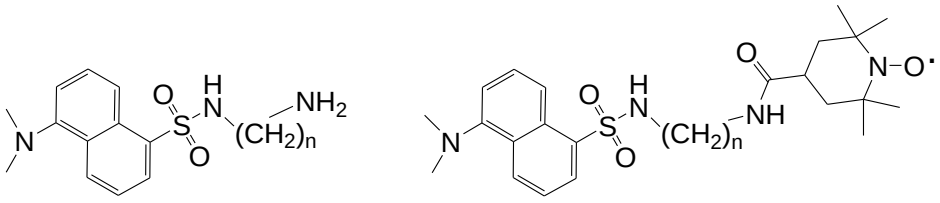

$DA_{1.n}$ **$DA_{1.n}T$**

Fig. 14. Molecular structures of mono and dual molecular probes $DA_{1.n}$ and $DA_{1.n}T$

EPR and fluorescence parameters of $DA_{1.n}T$ probes

The fluorescence probes $DA_{1.n}$ and $DA_{1.n}T$ are characterised by emission bands with maxima at ~540 nm and large widths (figure 15). The nitroxide group in the $DA_{1.n}T$ probes has a fast dynamic. The EPR line at high field is smaller in intensity than the other two lines. This can be explained by the linear molecular shape leading to a molecular motion that is not perfectly isotropic. The rotational correlation time increases with the increase of the alkyl chain, a common behaviour since this parameter is directly proportional to the hydrodynamic radius of the molecule and, implicitly, to the molecular weight. The values of the hyperfine splitting constant a_N are ~17.06 G, which indicates that the alkyl chain does not alter the polarity sensed by the nitroxide group.

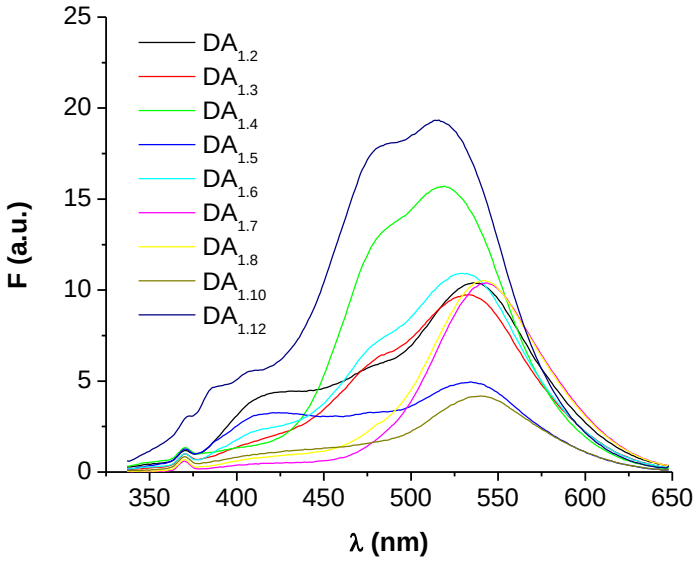

Fig. 15. Fluorescence spectra of $DA_{1.n}$ monomolecular probes

The spectral parameters of the dual molecular probes are given in tables 11 and 12.

Table 11. EPR parameters of $DA_{1.n}T$ probes in water

Probe	**$\tau\times10^{-10}$ (s)**	**a_N (G)**
$DA_{1.2}T$	0.72	17.1
$DA_{1.3}T$	0.77	17.1
$DA_{1.4}T$	0.84	17.1
$DA_{1.5}T$	0.91	17.1
$DA_{1.6}T$	0.86	17.1
$DA_{1.7}T$	0.96	17.1
$DA_{1.8}T$	1.05	17.1
$DA_{1.10}T$	1.20	17.1
$DA_{1.12}T$	1.40	17.1

Table 12. Fluorescence parameters of $DA_{1.n}$ and $DA_{1.n}T$ probes

	Φ		λ (nm)	
n	**$DA_{1.n}$**	**$DA_{1.n}T$**	**$DA_{1.n}$**	**$DA_{1.n}T$**
2	0,019	0,011	538	540
3	0,023	0,009	536	541
4	0,023	0,009	520	523
5	0,021	0,008	536	540
6	0,024	0,010	534	527
7	0,023	0,012	542	538
8	0,025	0,010	542	540
10	0,022	0,011	540	535
12	0,024	0,016	516	535

II.2.2. Interaction of $DA_{1.n}$ and $DA_{1.n}T$ with β-cyclodextrin

The interaction of the two series of probes, mono and dual molecular, with β-cyclodextrin was investigated using fluorescence spectroscopy in the former case and both fluorescence and EPR spectroscopies in the latter case. Starting from the assumption of a 1:1 stoichiometry, and considering the variation of the fluorescence intensity (figure 16) or of the rotational correlation time with the cyclodextrin concentration, we determined the values of the association constants. Both EPR and fluorescence lead to similar values of the association constants, which have the same order of magnitude with literature data for the interaction of dansyl derivatives with β-CD (10^2–10^3 M^{-1}) [21].

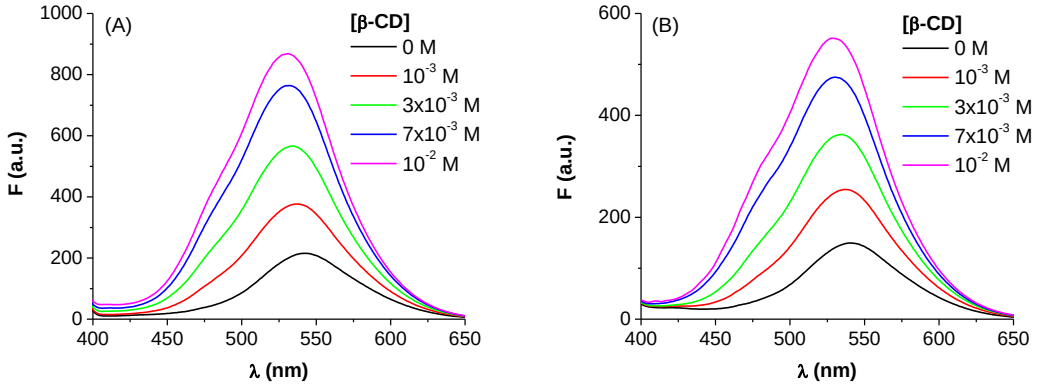

Fig. 16. Fluorescence spectra of (A) $DA_{1.7}$ and (B) $DA_{1.7}T$ in water, in the absence and in the presence of β-CD

II.3. Bis-dansyl fluorescence probes, $D_2A_{1.n}$

Fluorescent derivatives bearing two dansyl groups (figure 17) were obtained as by-products following the reaction of dansyl chloride with alkyl diamines.

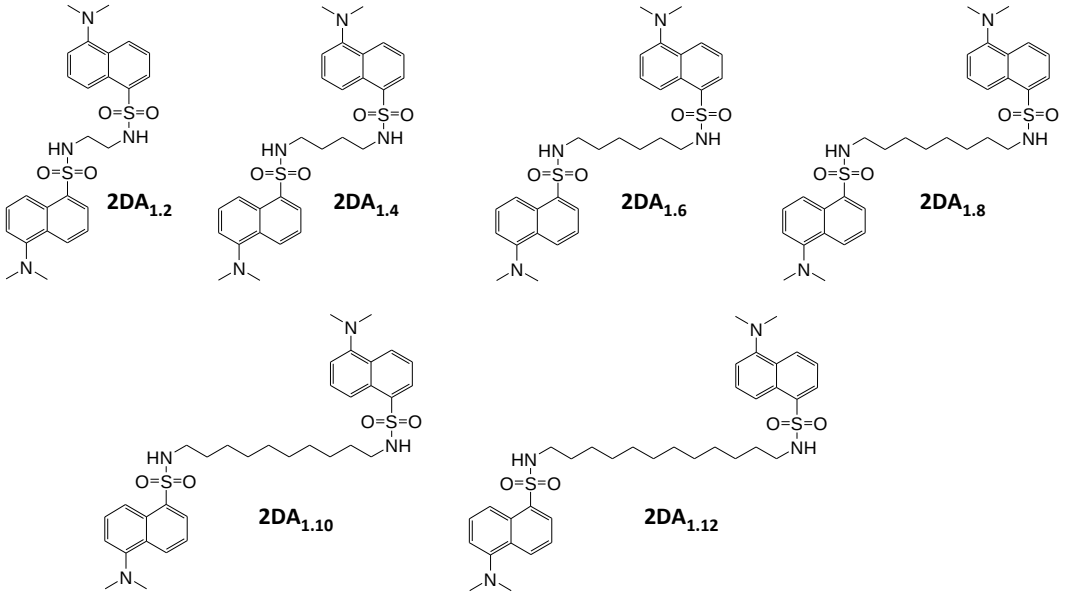

Fig. 17. Molecular structures of bis-dansyl fluorescent probes

II.3.1. Photophysical properties of the $D_2A_{1.n}$ fluorescence probes

The fluorescence spectra of bis-dansyl derivatives present an asymmetric emission band that originates in two emissive states due to the presence of two excited states – the normal excited state and a charge transfer excited state, with maxima at ~480 nm and ~520 nm, respectively. The length of the alkyl diamine chain has a significant influence on the emissive features of the $D_2A_{1.n}$ probes.

In table 15 we present the wavelengths of the absorption and fluorescence maxima of bis-dansyl derivatives in solvents of different polarity: water, ethanol, dichloromethane (DCM).

Table 15. Spectral parameters of the $D_2A_{1.n}$ bis-dansyl probes: emission wavelength (λ_f), relative magnitude (%A) and ratio of the surfaces of the two emission bands (A_{520}/A_{480})

Probe	**λ_f (nm)**			**%A**			**A_{520}/A_{480}**		
	water	**ethanol**	**DCM**	**water**	**ethanol**	**DCM**	**water**	**ethanol**	**DCM**
$D_2A_{1.2}$	522; 476	523; 476	516; 476	91.6; 8.4	96.3; 3.7	91.2; 8.8	10.9	26.0	10.4
$D_2A_{1.4}$	531; 470	522; 475	510; 474	90.1; 9.9	95.3; 4.7	93.0; 7.0	9.1	20.0	13.3
$D_2A_{1.6}$	510; 472	521; 475	509; 474	81.6; 18.4	95.0; 5.0	90.9; 9.1	4.4	18.9	10.0
$D_2A_{1.8}$	511; 472	520; 475	504; 473	80.6; 19.4	94.5; 5.5	94.8; 5.2	4.1	17.1	18.3
$D_2A_{1.10}$	507; 468	520; 475	510; 473	77.5; 22.5	94.3; 5.7	85.4; 14.6	3.4	16.5	5.8
$D_2A_{1.12}$	508; 468	520; 475	510; 473	75.7; 24.3	94.4; 5.6	85.4; 14.6	3.1	16.7	5.9

The change in the relative intensities of the two emission bands is much smaller in DCM (from $D_2A_{1.2}$ to $D_2A_{1.12}$, A_{520}/A_{480} decreases by only 43% in DCM as compared to a decrease of 72% in water) and is accompanied by a hypsochromic shift of 6 nm/3 nm. The effects are even less pronounced in ethanol, with a decrease in A_{520}/A_{480} of only 36% and a negligible hypsochromic shift (3 nm/1 nm).

The fluorescence quantum yield of the probes was determined according to the method described in the literature and applied to the other series of probes. In the case of the bis-dansyl derivatives, we also studied the influence of the solvent on the fluorescence intensity.

In water, the fluorescence quantum yield (Φ) is low for the probes with short chain ($D_2A_{1.2}$, $D_2A_{1.4}$) and long chain ($D_2A_{1.10}$, $D_2A_{1.12}$), but five to ten times higher for the probes with intermediary chain length ($D_2A_{1.6}$, $D_2A_{1.8}$). This effect is not observed in ethanol or DCM, where the probes have similar, high Φ values. Small Φ values (less than 0.1) have been reported for mono-dansyl derivatives in water and explained on the basis of high polarity and specific hydrogen bonding interactions that enhance the non-radiative decay pathways [22,23]. The lowering of the quantum yield due to an increased flexibility of the probes bearing long alkyl chains, which favours the non-radiative deactivation of the excited state, is a mechanism mentioned in the literature for other fluorophores as well [24]. Moreover, an intramolecular self-quenching mechanism, prompted by the aqueous environment, occurring between two fluorophores that are found in close vicinity cannot be excluded for short chain probes and for long chain probes that possess higher molecular flexibility.

II.3.2. Interaction of the $D_2A_{1.n}$ fluorescence probes with cyclodextrins

Three cyclodextrins (CD), namely β-CD, 2-hydroxypropyl-β-CD (2-HP-β-CD) and γ-CD, differing by the cavity size and solubility, were employed. The effect of the CD type on the emissive features of the $D_2A_{1.n}$ probes is depicted in figure 18.

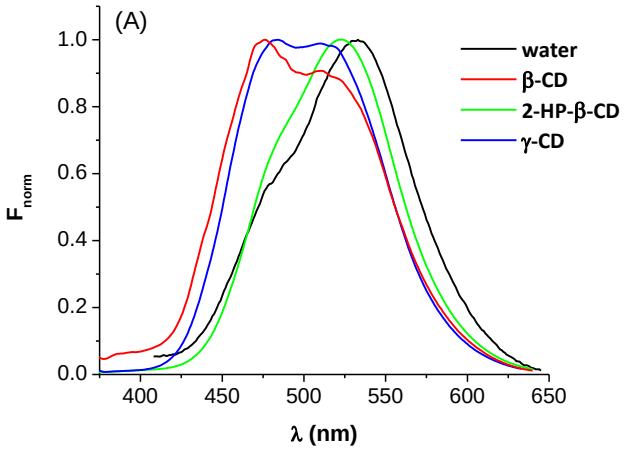

Fig. 18. Fluorescence spectra of $D_2A_{1.n}$ probes in cyclodextrin solution: (A) $D_2A_{1.4}$, $[D_2A_{1.n}] = 10^{-5}$ M, $[CD] = 10^{-2}$ M. The spectra have been normalized at the emission maximum

Upon interaction with CDs a hiperchromic shift of the emission band was observed for all $D_2A_{1.n}$ probes except $D_2A_{1.6}$ and $D_2A_{1.8}$. the fluorescence increase can be explained by the less polar medium sensed by the probe in the presence of CD. We have shown that the Φ values of the $D_2A_{1.n}$ probes, where = 2, 4, 10 şi 12, increase on going from water to a les polar solvent. The decrease in micropolarity around the dansyl group and the steric restrictions imposed by the CD cavity favour an increase in the Φ value [23]. The fluorescence decreased observed for $D_2A_{1.6}$ and $D_2A_{1.8}$ cannot be explained by the same mechanism, since these two probes have similar Φ values in water and in ethanol. It is well known that the polarity of the CD cavity is close to that of ethanol [24]. In the case of these probes, a different complexation mode is inferred in which a bent conformation of the alkyl chain is favoured, which brings in close proximity the two dansyl moieties and leads to self-quenching.

In the presence of 2-HP-β-CD, all probes yield similar spectra in terms of band position and band shape. Among the three CDs considered in this study, the influence of the linker length

is minimal in 2-HP-β-CD. As the linker length increases, the shoulder at 480 nm becomes more pronounced and a small hypsochromic shift (3 nm) of the charge transfer band is recorded.

Table 20. Spectral parameters of the $D_2A_{1.n}$ bis-dansyl probes in 10^{-2} M cyclodextrin solution, as obtained by deconvolution

Sondă	**λ_f (nm)**				**A_{520}/A_{480}**			
	apă	**β-CD**	**2-HP-β-CD**	**γ-CD**	**apă**	**β-CD**	**2-HP-β-CD**	**γ-CD**
$D_2A_{1.2}$	522; 476	513; 476	522; 471	527; 468	10.9	6.3	11.4	5.8
$D_2A_{1.4}$	531; 470	520; 465	522; 473	515, 468	9.1	2.1	13.3	3.7
$D_2A_{1.6}$	510; 472	510; 470	521; 472	515; 468	4.4	3.4	10.6	3.2
$D_2A_{1.8}$	511; 472	517; 468	519; 472	518; 469	4.1	2.4	9.0	2.6
$D_2A_{1.10}$	507; 468	509; 470	519; 471	508; 467	3.4	4.4	9.7	4.0
$D_2A_{1.12}$	508; 468	508; 469	519; 472	510; 468	3.1	3.6	5.0	3.9

Markedly different spectral features from those in 2-HP-β-CD are observed in the presence of β-CD and γ-CD. This ability of the $D_2A_{1.n}$ probes to distinguish between different types of molecular hosts may find further application in probing supramolecular systems containing CDs. The emission spectra in β- and γ-CD resemble those of the long chain probes in water, having A_{520}/A_{480} ~ 3. Considerable hypsochromic shifts of 10 nm with respect to water are recorded at 10^{-2} M β-CD concentration for $D_2A_{1.2}$ and $D_2A_{1.4}$, and a hypsochromic shift of 16 nm is recorded at 10^{-2} M γ-CD concentration for $D_2A_{1.4}$ (Table 20).

All the experimental findings discussed above on the emissive properties of the bis-dansyl molecular probes and their interaction with cyclodextrins point out the great sensitivity of the $D_2A_{1.n}$ probes to the microenvironmental properties. Therefore, these probes can be further used for investigating other non-uniform systems at nanoscale level, including self-assembled systems like gels and polymeric micelles.

In conclusion, we found that the charge transfer excited state is favoured in short chain $D_2A_{1.n}$ probes (n = 2, 4), while the normal state is stabilized in long chain probes (n = 6, 8, 10, 12). Moreover, the dual emission of the $D_2A_{1.n}$ probes is tunable by changing the polarity of the environment. This feature differentiates these compounds from currently employed monodansyl polarity probes and recommends the use of $D_2A_{1.n}$ bis-dansyl probes in solvatochromic applications as a means to measure a system's micropolarity, based on the value of the

normal/charge transfer ratio. The $D_2A_{1.n}$ probes can also be of use in probing supramolecular systems containing CDs, due to the different spectral response of the probes in terms of band position and LE/CT ratio, and hence their ability to distinguish between different types of (macro)molecular hosts [25].

CONCLUSIONS AND PERSPECTIVES

The results presented and discussed in this thesis pointed out to two new series of derivatives with dual properties that can be used in various fields of chemistry referring to non-covalent interactions in supramolecular systems and in the investigation of diffusion processes and chemical reactions.

The newly synthesised dual molecular probes present fluorescent as well as paramagnetic properties. The studies have shown that the chemical nature of the structural unit connecting the fluorescent and paramagnetic groups can govern the interactions of the probe with other species. The emission and, in certain cases, the paramagnetic properties do not vary linearly with the length of the flexible linker among a series of compounds. As an example, in the case of the dual probes bearing oligo-ethylene glycol linkers, the variation of the rotational correlation time and fluorescence quantum yield are determined by the preferential conformation of the C-C and C-O bonds forming the oligo-ethylene glycol chain.

Moreover, the particularities of the host molecule determine the geometry of the resulting supramolecular structures. In the case of the $Py(EG)_nT$ dual probes, the oligo-ethylene glycol chains interact with cyclodextrins resulting, most probably, in sandwich-like complexes. These dual probes have been used to evidence their diffusion in covalent polymeric gels, and also to study the formation of thermotropic gels in systems containing the block-copolymer Pluronic F127. The behaviour of the dual probes $Py(EG)_nT$ in Pluronic F127 systems was compared with the behaviour of monomolecular fluorescent $Py(EG)_n$ or paramagnetic $(EG)_nT$ probes. The results have indicated that the probes having fluorescent properties, $Py(EG)_nT$ and $Py(EG)_n$, do not possess high sensitivity towards the micropolarity changes accompanying the phase transition from micelle to gel in systems containing F127. Differently, the paramagnetic probes

are much more suited for the study of this transition, due to the fact that the hyperfine splitting constant is a parameter much more sensitive to polarity changes.

We consider that the results referring to dual molecular probes can be completed with other results regarding the dual probe behaviour in supramolecular systems containing polymeric structures.

In what concerns the second series of dual molecular probes, $DA_{1.n}T$, in which the fluorescent dansyl group is connected to the paramagnetic TEMPO group by alkyl chains, the results led to the conclusion that the interaction with cyclodextrins occurs *via* the dansyl group. Monodansyl ($DA_{1.n}$) and bis-dansyl ($D_2A_{1.n}$) derivatives have been obtained as by-products and characterised from a physico-chemical point of view. The association constants characterising their inclusion complexes with cyclodextrins have also been determined.

Future studies can involve the synthesis of new dual molecular probes with affinity for metallic nanoparticles such as those of gold or silver. Moreover, the redox properties and spin trapping properties of these molecules can be studied in systems in which unstable free radicals are generated.

References

[1] I. E. Valdez-Orozco, S. M. Rojas-Montoya, M. Vonlanthen, E. Rodriguez-Alba, G. Burillo, E. Rivera, *Rad. Phys. Chem.*, **2018**, 153, 226–233.

[2] M. Bohorquez, C. Koch, T. Trygstad, N. Pandit, *J. Colloid Interf. Sci.*, **1999**, 216, 34–40.

[3] P. Alexandridis, T. A. Hatton, *Colloids Surf. A: Physicochem. Eng. Aspects*, **1995**, 96, 1–46.

[4] N. B. Elliott, T. NdouIsiah, M. Warner, *J. Incl. Phenom. Mol. Recogn. Chem.*, **1993**, 16, 99–112.

[5] A. Nakajima, *Bull. Chem. Soc. Jpn.*, **1971**, 44, 3272–3277.

[6] K. Kalyanasundaram, J. K. Thomas, *J. Am. Chem. Soc.*, **1977**, 99, 2039–2044.

[7] C. Yao, H. B. Kraatz, R. P. Steer, *Photochem. Photobiol. Sci.*, **2005**, 4, 191–199.

[8] M. Marek, K. Kaiser, H. J. Gruber, *Bioconjugate Chem.*,**1997**, 8, 560–566.

[9] A. Hashidzume, Y. Zheng, A. Harada, *Beilstein J. Org. Chem.*, **2012**, 8, 1312–1317.

[10] G. Ionita, V. Meltzer, E. Pincu, V. Chechik, *Org. Biomol. Chem*., **2007**, 5, 1910–1914.

[11] L. X. Song, L. Bai, X. M. Xu, J. He, S. Z. Pan, *Coord. Chem. Rev.*, **2009**, 253, 1276–1284.

[12] G. Ionita, V. Chechik, *Chem. Commun.*, **2010**, 46, 8255–8257.

[13] G. Ionita, A. M. Ariciu, I. M. Turcu, V. Chechik, *Soft Matter*, **2014**, 10, 1778–1783.

[14] L. C. Cesteros, C. A. Ramirez, A. Pecina, I. Katime, *J. Appl. Polym. Sci*., **2006**, 102, 1162–1166.

[15] L. C. Cesteros, C. A. Ramirez, A. Pecina, I. Katime, *Macromol. Chem Phys.*, **2007**, 208, 1764–1772.

[16] S. Mocanu, I. Matei, S. Ionescu, V. Tecuceanu, G. Marinescu, P. Ionita, D. Culita, A. Leonties, G. Ionita, *Phys. Chem. Chem. Phys.*, 2017,19, 27839–27847.

[17] G. Ionita, G. Marinescu, C. Ilie, D. F. Anghel, D. K. Smith, V. Chechik, *Langmuir*, **2013**, 29, 9173−9178.

[18] P. Alexandridis, B. Lindman, Amphiphilic Block Copolymers: Self-Assembly and Applications, Elsevier: Amsterdam, **2000**.

[19] P. Alexandridis, *Curr. Opin. Colloid Interface Sci.*, **1996**, 1, 490–501.

[20] R. Baratoiu, S. Mocanu, I. Matei, M. Bem, E. Hristea, V. Tecuceanu, G. Ionita, *Macromol. Chem. Phys.* 2019, 220, articol nr. 1800489.

[21] M. V. Rekharsky, Y. Inoue, *Chem. Rev.*, **1998**, 98, 1875–1917.

[22] S. Sharma, A. Gupta, C. P. Pradeep, A. Dhir, *ChemistrySelect*, **2017**, 2, 10517–10523.

[23] Y. B. Ruan, A. Depauw, I. Leray, *Org. Biomol. Chem.*, **2014**, 12, 4335–4341.

[24] A. Heredia, G. Requena, F. Garcia Sanchez, *J. Chem. Soc. Chem. Commun.*, **1985**, 1814–1815.

[25] S. Mocanu, G. Ionita, S. Ionescu, V. Tecuceanu, M. Enache, A. R. Leonties, C. Stavarache, I. Matei, *Chem. Phys. Lett.*, 2018, 713, 226–234.